AIP | The Journal of Chemical Physics

# Influence of surface vacancy defects on the carburisation of Fe 110 surface by carbon monoxide

Aurab Chakrabarty, Othmane Bouhali, Normand Mousseau, Charlotte S. Becquart, and Fedwa El-Mellouhi

Citation: The Journal of Chemical Physics **145**, 044710 (2016); doi: 10.1063/1.4958966
View online: http://dx.doi.org/10.1063/1.4958966
View Table of Contents: http://scitation.aip.org/content/aip/journal/jcp/145/4?ver=pdfcov
Published by the AIP Publishing



# Influence of surface vacancy defects on the carburisation of Fe 110 surface by carbon monoxide

Aurab Chakrabarty,[1,a)] Othmane Bouhali,[1] Normand Mousseau,[2] Charlotte S. Becquart,[3] and Fedwa El-Mellouhi[4,b)]
[1]*Texas A&M University at Qatar, P.O. Box 23874, Doha, Qatar*
[2]*Département de Physique and RQMP, Université de Montréal, Case Postale 6128, Succursale Centre-Ville, Montréal (QC) H3C 3J7, Canada*
[3]*UMET, UMR CNRS 8207, ENSCL, Université Lille I, 59655 Villeneuve d'Ascq cédex, France*
[4]*Qatar Environment and Energy Research Institute, Hamad Bin Khalifa University, P.O. Box 5825 Doha, Qatar*

(Received 11 April 2016; accepted 1 July 2016; published online 29 July 2016)

Adsorption and dissociation of gaseous carbon monoxide (CO) on metal surfaces is one of the most frequently occurring processes of carburisation, known as primary initiator of metal dusting corrosion. Among the various factors that can significantly influence the carburisation process are the intrinsic surface defects such as single surface vacancies occurring at high concentrations due to their low formation energy. Intuitively, adsorption and dissociation barriers of CO are expected to be lowered in the vicinity of a surface vacancy, due to the strong attractive interaction between the vacancy and the C atom. Here the adsorption energies and dissociation pathways of CO on clean and defective Fe 110 surface are explored by means of density functional theory. Interestingly, we find that the O adatom, resulting from the CO dissociation, is unstable in the electron-deficit neighbourhood of the vacancy due to its large electron affinity, and raises the barrier of the carburisation pathway. Still, a full comparative study between the clean surface and the vacancy-defected surface reveals that the complete process of carburisation, starting from adsorption to subsurface diffusion of C, is more favourable in the vicinity of a vacancy defect. *Published by AIP Publishing.* [http://dx.doi.org/10.1063/1.4958966]

## INTRODUCTION

Point defects such as vacancies and interstitials are the most abundant form of atomic-scale disorders that can significantly alter the material properties. Vacancy defects in metals can be formed in a number of ways, but mostly appear during solidification, and are of vital importance in deciding key chemical and structural properties of the metal and its alloys. Single vacancy defects are known for affecting atomistic position, migration and segregation of other impurity atoms such as C, Cr, and Mn, that are common components in steels,[1–3] or H, He, N, O that are unwanted impurities.[3–5] Vacancy defects are also known for self-segregation, leading to voids that act as trap centres for alloying atoms and pinning centres for larger defects such as dislocations and affects the overall structural properties.[6–8] Positron annihilation spectroscopy experiments reveal that the single Fe vacancies can be mobile at room temperature and migrate through the crystal to form a vacancy cluster or supervacancy, predominantly in the presence of hydrogen.[1] This migration is driven by the lower defect formation energy at the edge of a void with respect to bulk.[6,9] A lower formation energy at a surface means that the net flux for vacancy defects will be from the bulk to nearby surfaces or voids. This assumption leads us to question the role of vacancy defects on the metal-hydrocarbon catalytic reactions, a topic that has not been much studied until now. Reaction of CO with Fe surfaces is observed at an elevated temperature, between around 700 and 1100 K, resulting in the carburisation of the surface by dissociation of CO and diffusion of C through the surface.[10,11] C atoms tend to segregate in the metal to form a metastable cementite ($Fe_3C$) phase and Fe atoms diffuse into cementite and erupt as Fe metal dust,[11,12] therefore depleting the structural integrity of the metal. This phenomenon is known as metal dusting corrosion (MDC) and is a severe material failure that occurs to Fe and its alloys exposed to hydrocarbons in high temperatures.

From an atomistic modeling perspective, carburisation of Fe surface by CO can be viewed as the result of three consecutive processes, i.e., adsorption and dissociation of CO molecule on Fe surface,[10,13–15] followed by diffusion of C atoms from surface to subsurface.[16] Adsorption is an exothermic process where the CO molecule gets attached to the Fe surface by a metallic bond between the Fe and the C atom.[14,17] Dissociation, on the other hand, is an endothermic process that requires breaking a C–O triple bond, a process associated with an average dissociation energy of 11.2 eV per molecule in vacuum.[18] The metal surface acts as a catalyst to break this bond at a much lower energy threshold.[12] Earlier density functional studies show that on Fe-110 surface, the CO dissociation barrier is ~1.5 eV.[14,15] However, a number of experiments suggest that the dissociation barrier may be even lower in practice as an onset temperature as low as 380 K is observed for dissociation to occur.[19–21] This may be associated with complex reaction pathways as a

a)aurab.chakrabarty@qatar.tamu.edu
b)felmellouhi@qf.org.qa

number of other molecules and sites that could act as an activator, such as H and other reactive hydrocarbons that are generally present and could assist the dissociation process.[22] An extensive *ab initio* study on the water-gas shift reactions by Liu *et al.*[15] has shown that the Fe-110 surface precovered with H, O and OH reduces dissociation of CO in comparison to a clean surface. Instead, the hydrogenation of CO was found to be accelerated in a precovered surface. However, in order to explain carburisation and metal dusting from CO,[12] the dissociation of CO and surface to subsurface diffusion of C must be understood. In an early work, Jiang *et al.* have calculated the adsorption and dissociation of CO on Fe surfaces. This topic has been revisited by a number of recent works.[23–27] While a dense CO-coverage (≤0.25 monolayer) is commonly considered, we have shown that the dissociation barrier is greatly reduced at a dilute coverage (up to 0.0625 monolayer),[28] due to the unrestricted relaxation of the Fe lattice. However, the presence of intrinsic defects is a likely candidate that can significantly affect the carburisation process and has not been considered yet. Here, we show a characterisation study of a single vacancy defect on the surface and its effect on the electronic mechanism of the dissociation process. Furthermore, we show that a vacancy defect does not only affect the dissociation of CO but also assists the surface to subsurface diffusion of carbon, which is the next step in carburisation. A comparison with the surface-to-subsurface diffusion of C on the clean surface calculations as well as that in the literature[16] reveals that the surface vacancy defects act as activator sites for both dissociation and diffusion of C. Studies on interaction of the vacancy defect and interstitial impurities suggest that the vacancy defect and interstitial C are strongly attracted to each other and forms a C-vacancy complex.[5] A recent kinetic Monte-Carlo study on the dynamics of the C-vacancy complex using the off-lattice kinetic activation-relaxation technique shows that the complex can migrate with a barrier of 1.5 eV[29] but the dissociation of this complex requires a similar amount of energy. Therefore migration of the whole complex takes place by going through numerous small barriers involving dissociation and reassociation of the complex. A literature survey on more recent works using standard GGA PW91[30] and PBE[31] functionals and meta-GGA, PKZB,[32] RPBE[33] approximations reveal that the exact adsorption energy on particular sites depends heavily on the choice of the exchange-correlation functional.[14,34,35] Modern functionals tend to yield a consistent relative energy between adsorption energies at different sites, in agreement with a number of experimental parameters such as vibrational frequencies and work function changes for CO adsorption.[14] To explore the dissociation, the nudged elastic band (NEB)[36] method with PBE-GGA exchange-correlation functional has proven to be a reliable tool that can predict the minimum-energy reaction path.[10,13,14]

Over the past decade, extensive studies of the atomistic characteristics of the vacancy defect in $\alpha$-iron using density functional theory have demonstrated the importance of *ab initio* calculations for understanding the kinetics of defects at the surface as well as in bulk systems.[2,37–40] In this work we follow these approaches to characterize a single vacancy defect on the Fe-110 surface and study its role in the adsorption and dissociation of CO. The formation energy of such a vacancy defect is calculated and is found to be 0.87 eV, which is much lower than that in the bulk (1.9-2.2 eV[5,39]). This suggests frequent abundance of single vacancy defects on the surface. With the introduction of a vacancy, the adsorption of the CO molecule will move to a different low-energy adsorption site, therefore all the new high-symmetry sites must be explored. Depending on the initial adsorption site, the dissociation path is assumed to be different as well. It is observed that the adsorption of CO is energetically favourable at sites in the vicinity of a vacancy defect. With the prior knowledge that the C interstitial in bulk Fe has a strong affinity to vacancy defects, it is anticipated that the defect will significantly affect the dissociation mechanism of CO. We show here that the binding energy between a C atom as surface adatom and a single vacancy defect on the 110 surface is as high as 1.7 eV. Since the defect presence should induce a complex dissociation path, we search for the minimum energy dissociation path, based on the knowledge of the geometry relaxation of the defect. The nudged elastic band method is used to determine the minimum energy path which requires prior knowledge of the initial and final configurations. With no prior information on the state at the end of the dissociation process, we must guess a likely dissociation path from the experience with the clean surface and analyze the electronic mechanism of the dissociation process carefully to obtain the minimum-energy dissociated configuration. We find that the single vacancy defect reduces the dissociation barrier in comparison to a clean surface. Additionally it allows the C atom to penetrate into the subsurface layer. However, the reduction in the dissociation barrier caused by the vacancy is much smaller than the C-vacancy binding energy. Analysis of the electronic charge density-dynamics during the dissociation and diffusion process indicates that the O atom has a significant role to play in the dissociation of CO in the presence of a vacancy and subsurface diffusion of C. In particular, the large electron affinity of O atom restricts C–Fe bond formation in the electron-deficit vicinity of the vacancy, even when the CO molecule is completely decomposed. Therefore the O atom is unstable as an adatom itself near the vacancy and drags the C atom away from the vacancy. This effect competes with the C-vacancy interaction, eventually raising the dissociation barrier.

## COMPUTATIONAL METHODS

DFT calculations are performed using PBE-GGA exchange-correlation functional with the plane-wave basis pseudo-potential method implemented in the Vienna *ab initio* simulation package (VASP).[41] Total energies are calculated with a kinetic energy cutoff fixed at 400 eV for all calculations. Grimme's DFT-D2[42] method was used to incorporate van der Waals interactions. Convergence criteria of $10^{-6}$ eV/atom and $10^{-3}$ eV/Å were selected for total energy and structure relaxation, respectively. A ferromagnetic (FM) bcc structure with space group $Im\bar{3}m$ was used for bulk Fe. The equilibrium bulk lattice constant was found to be 2.831 48 Å.

This is well in agreement with previous *ab initio* results (2.83 Å),[5,39,43] as well as experiment (2.86 Å).[44]

For the 110 surface a $4 \times 4 \times 10$ simulation box is created using this bulk lattice constant. The surface is constructed using a 13-layer thick slab with 11 Å of vacuum. Previous work with PAW-PBE pseudo-potential method confirmed that a vacuum of 10 Å is adequate as the interaction between slabs due to the periodic boundary condition is negligible.[28,45,46] The top four layers are free to relax in all 3 dimensions. The next two layers are free to relax only in the direction perpendicular to the surface while the remaining layers are kept fixed with atoms in their ideal positions. In an earlier work we have shown that the 110 surface is highly stable with minimum reconstruction associated.[28] Only the atoms in the top 3 layers are displaced. Therefore for computationally demanding calculations such as dissociation barriers, we select a $4 \times 4$, 7-layer thick supercell with 112 atoms and 16 Å of vacuum. The top three layers are allowed to relax freely while the next two layers are allowed to displace along the c axis, perpendicular to the surface and the rest are kept frozen. The surface energy, reconstruction parameters, and adsorption energies for CO are compared with the 13-layer thick supercell and we find no energy difference within a 0.1 meV tolerance. A K-point mesh is automatically generated using Monkhorst-Pack grid. For the adsorption calculations a $7 \times 7 \times 1$ grid is used while we choose a coarser $5 \times 5 \times 1$ grid for the dissociation minimum energy path.

The adsorption energy is calculated using

$$E_{ads}^{S} = E_{TOT}^{\mathrm{CO}-surf} - E_{TOT}^{cln}(\mathrm{CO}), \tag{1}$$

where $E_{TOT}^{\mathrm{CO}-surf}$ and $E_{TOT}^{cln}(\mathrm{CO})$ are the total energies corresponding to a CO-adsorbed surface and a clean surface with a CO molecule placed in the vacuum away from the surface, respectively.

The climbing-image nudged elastic band (CI-NEB) method[36] implemented in VASP is used to trace the minimum energy paths (MEP). In order to find a transition state, the end-point (initial and final) configurations for the reaction are fully relaxed with high precision. As input, NEB uses an interpolated chain of intermediate configurations between the two end point configurations, connected by springs. The whole chain is then relaxed simultaneously with a fixed spring constant until the total average force minimizes under the tolerance limit of 0.01 eV/Å. In this work, 15 intermediate configurations or images are considered, starting from an on-top adsorbed to a fully dissociated configuration. The MEPs are obtained with a three-stage high-precision relaxation of the path with CI introduced in the 2nd stage of relaxation such that the saddle point is obtained accurately, yet no small detail of the reaction path is missed.

## RESULTS

### Surface vacancy

Single vacancy defects are expected to form on the surface due to the low defect formation energy. A quick set of calculations reveals that the formation energy of a single vacancy defect on the surface is less than 1 eV. However, for a precise value of the formation energy, the unwanted energy contribution from the periodic boundary condition must be eliminated. This is done by converging the vacancy formation energy with different supercells with increasing surface area. One must compromise between the precision and computational cost for these calculations. Details of this estimation are given in Appendix A, which shows the difficulty to overcome in the work with point defects in surface systems. The $4 \times 4$ surface is used for all calculations, under the assumption that the change in vacancy formation energy dropped below 0.01 eV. For this system, the formation energy of a single surface vacancy is computed to be 0.87 eV. This is much lower than the computationally derived formation energy of a bulk vacancy which ranges from 1.9 eV[38] to 2.2 eV[39] depending on the model, while positron annihilation spectroscopy experiments suggest a value of 1.5 eV for pure Fe[47] and 2 eV for carbon steels.[48] The deformation caused by the defect is small and is shown in Figure 1.

### Adsorption

For the adsorption of a CO molecule on the 110 surface, we consider all symmetrical adsorption sites: the on-top, hollow, bridge, and quasi-threefold sites. For a surface with a vacancy, we concentrated on the same symmetric sites at the immediate vicinity of the vacancy. The adsorption sites are shown in Fig. 2. Table I shows the corresponding adsorption energies.

For a clean surface, the on-top position is energetically the most favourable adsorption site. The CO molecule sits upright with the C atom closer to the Fe surface (Fig. 2) in all three symmetric sites. The C–O bond (1.17 Å in vacuum) is stretched by 4.5%–9.1% with the largest stretch for the hollow site. The CO molecule relaxes to a position where the C atom is 0.9 Å above the surface. In the case of a vacancy, the CO molecule prefers to hover above a quasi-threefold site next to the vacancy. The molecule is tilted by an angle of 34° from the perpendicular to the surface towards the vacancy. Interestingly, being on the quasi-threefold site, instead of forming bonds with the three nearest neighbour Fe atoms, the C atom forms a bond with one Fe atom along the axis of the molecule. Fig. 3 shows the charge density isosurface

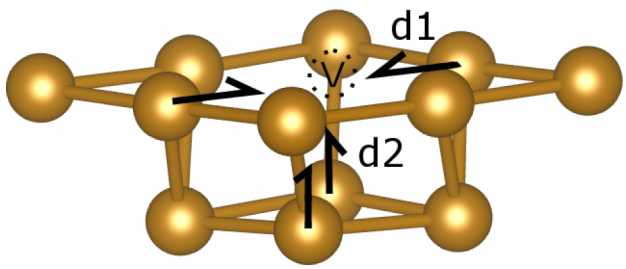


FIG. 1. Deformation of the local structure around a surface vacancy defect on the 110 surface. The deformation of nearest neighbour Fe atoms to the vacancy V on the same layer and the next is depicted with the arrows with magnitude d1 = 1.1% and d2 = 0.6%, respectively.

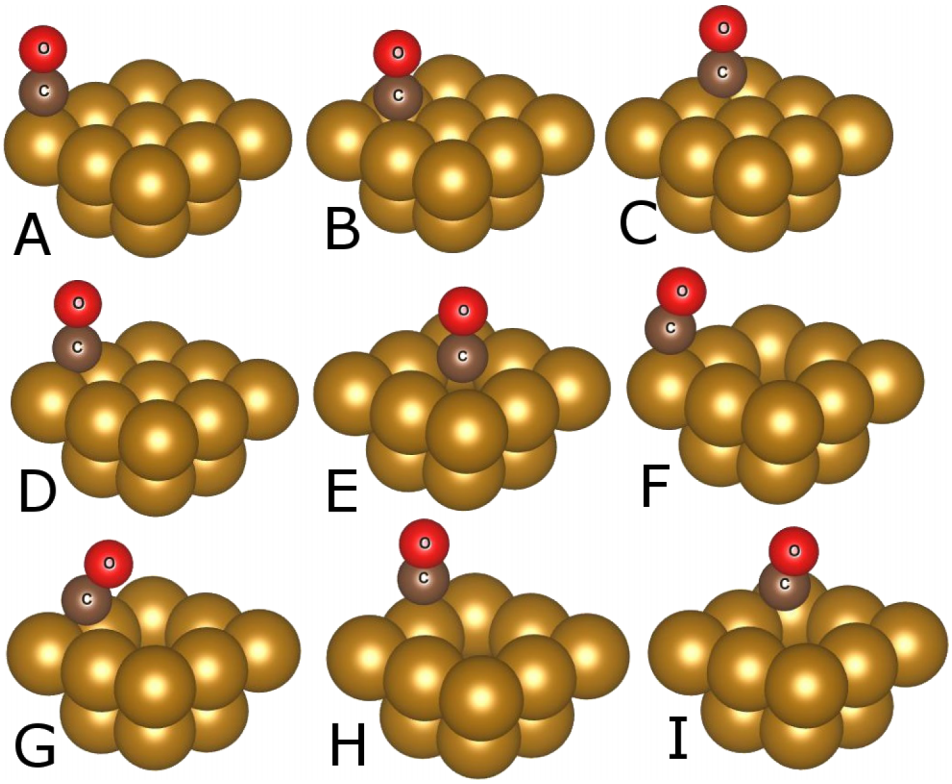


FIG. 2. Different adsorption sites for CO on Fe-110 surface. A: on-top; B: hollow; C: bridge; D: quasi-threefold; E: vacancy; F: vacancy-on-top; G: vacancy-quasi-threefold; H: vacancy-nearest neighbour on-top; and I: vacancy-bridge. The corresponding adsorption energies are listed in Table I.

of the tilted CO-adsorbed configuration. Note that due to the high electron affinity of the oxygen, the s-p electron cloud is skewed towards the O atom and causes the p orbital along the axis of the molecule to be most electron-rich. The electron-rich p orbital makes a bond along the axis of the molecule more favourable. This explains why the upright configuration on the on-top site is the most stable for a clean surface. Note that this is the case for molecular adsorption of CO as an isolated phenomenon. There are evidences of a skewed or bridge-site adsorptions for high CO coverages.[14,17] In the presence of a vacancy, however, a tilted configuration of the molecule is more favourable. The strong affinity of C to the vacancy compensates the electron deficit created by the vacancy and therefore an adsorption site at the edge of the vacancy is the most stable adsorption configuration. The C atom is 1.5 Å above the quasi-threefold site and 1.77 Å from the nearest Fe atom. The C–O bond is stretched to 1.18 Å. The hollow site next to the vacancy is right next to the quasi-threefold site and the adsorption energy differs by 10 meV only.

The adsorption energies for the clean surface are slightly larger in comparison with the ones calculated in previous work which are in the range of 1.7-2.0 eV.[14,15,17] We have shown in an earlier work[28] that this small advantage in adsorption is facilitated by a dilute coverage with negligible van der Waals repulsion between the neighbouring CO molecules. As for the surface with vacancy defect, an adsorption site in a close vicinity of the vacancy such as the one right into the vacancy and the bridge site next to it have thermodynamically less favourable adsorption energies and are unstable. This is due to the local electron deficit due to the vacancy defect which is unfavourable to bind the CO molecule to the surface. However, the on-top sites are energetically more attractive than the bridge and vacancy sites, due to their ability of forming sp bonds with the C atom as

TABLE I. Adsorption energies of CO molecules at different surface adsorption sites. All energies are given in eV.

| Clean surface | | | | | |
|---|---|---|---|---|---|
| On-top | Hollow | Bridge | QTF[a] | | |
| −2.12 | −2.09 | −1.90 | −2.07 | | |
| Surface with vacancy defect | | | | | |
| On-top′[b] | Hollow | Bridge | QTF | On-top″[c] | Vacancy |
| −2.00 | −2.24 | −1.57 | −2.25 | −2.22 | −1.66 |

[a]Quasi-threefold.
[b]On-top, nearest neighbour to the vacancy.
[c]On-top, 2nd nearest neighbour to the vacancy.

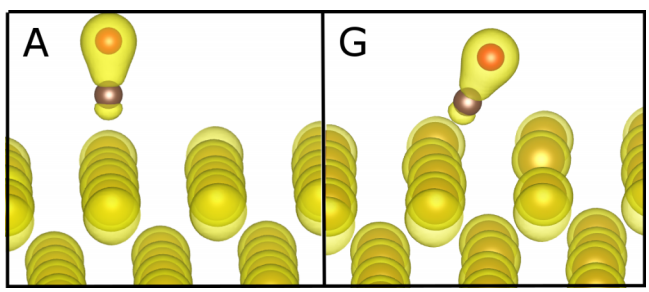


FIG. 3. Charge density isosurface of CO molecule adsorbed on the 110 surface. A: Clean surface and G: surface with vacancy are labelled according to Figure 2.

described above. The influence of this large electron-affinity of the O atom on the adsorption process is overviewed in the section titled "Discussion" from an electronic structure perspective.

### Dissociation

Once the CO molecule is adsorbed on the surface, it decomposes into surface-adsorbed C and O atoms and the C atom diffuses into the Fe surface to complete the carburisation process. The climbing-image nudged elastic band method is used to estimate the minimum energy paths associated with dissociation of CO and diffusion of C into subsurface. We use the on-top site as initial configuration for dissociation, which was found to be the most stable condition for adsorption and for the clean surface. The final configuration consists of the CO molecule completely decomposed into C and O adatoms on the surface. According to earlier investigations,[14,49] upon decomposition, the most stable positions for C and O atoms correspond to the two neighbouring hollow sites shown as configuration D in Fig. 4. In this dissociated configuration the C atom sinks 0.3 Å below the surface while the O atom sits at 0.7 Å above the surface. The total energy of the final configuration is 0.72 eV lower than the initial configuration. In an earlier work, we have shown that, along with the adsorption energies, the energetics of these final configurations are strongly affected by the CO coverage ratio and the size of the simulation box.[28] Higher coverages, due to the restricted relaxation of the lattice upon C-insertion, result in higher dissociation barriers. Here we use a $4 \times 4$ periodic surface with CO coverage of 0.0625 ML for all calculations so that a comparison can be made between a clean surface and a surface with a vacancy defect.

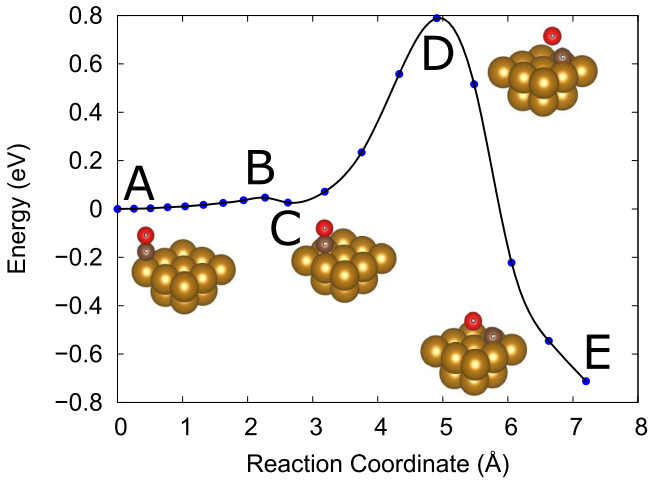


FIG. 4. Minimum energy path for CO-dissociation on clean Fe-110 surface. Important intermediate configurations are shown. A—Initial minimum: on-top adsorbed CO. B—Transition state for molecular migration of CO. C—Local minimum: Hollow site-adsorbed CO. D—Saddle point, CO bond severing. E—Decomposed into surface-adsorbed C and O atoms. Note that the barrier energy is much smaller than that reported in earlier works (~1.5 eV).[14,15] We have shown in an earlier work[28] that the barrier is reduced drastically in a dilute coverage of 0.0625 ML that is adopted in this work. This reduction is due to the unrestricted relaxation of the Fe lattice upon C insertion.

Dissociation of CO in the presence of a surface vacancy defect is more complex than that on the clean surface. The vacancy removes the symmetry and opens up a number of possible dissociation paths within a narrow spectrum of energy barriers and transition states. In order to obtain the minimum energy dissociation path, it is necessary to consider the minimum energy initial and final configurations. According to Table I the quasi-threefold site near the vacancy is associated with the lowest adsorption energy and therefore must be chosen as the initial configuration. The final configuration, however, is not as intuitive as it is for the clean surface. Based on our experience with dissociation on the clean surface, it is assumed that in the final, dissociated configuration in the presence of a vacancy, the decomposed C and O atoms should occupy a symmetric site similar to that on a clean surface, i.e., with the C atom in the hollow site, next to the vacancy and the O atom above another hollow site. In practice, however, this does not represent the dissociated minimum-energy configuration. We have stated in the section titled "Adsorption" that the large electron affinity of the O atom does not favour the electron-deficit vicinity of the vacancy and is more stable away from the vacancy. The C atom, on the other hand, gets trapped by the vacancy. The binding energy between a surface vacancy and a lone C surface adatom is estimated to be 1.7 eV with respect to an on-top site (see the section titled "Discussion"). Therefore, following dissociation, the C atom proceeds to jump into the vacancy pit. The most stable dissociated configuration can be found by placing the O atom away from the vacancy and the C atom in the vacancy, yet within the limit of a reasonable reaction coordinate such that the displacement of the atoms from the initial configuration is not too large. The dissociated minimum-energy configuration thus obtained is 0.66 eV lower than the initial quasi-threefold adsorbed configuration and is depicted in Figure 5. The initial part of the dissociation mechanism is similar to that on a clean surface. The CO molecule migrates to a less stable adsorption site next to the vacancy, in this case, the nearest neighbour on-top site 0.24 eV higher in energy shown as configuration C, and by crossing a 0.38 eV barrier at B shown in Figure 5. From this metastable adsorption site, the system has to climb a further 0.39 eV saddle point (D) for dissociation before settling down into the low energy dissociated state E. At the transition state, the strong C-vacancy attraction allows the C–O bond severing at a lower energy. However, the O atom gets separated from the CO molecule by claiming electrons from the densely packed surface. In the vicinity of the vacancy, these electronic charges must be supplied from the shallow energy levels associated with the C–Fe bond, thus weakening the C–Fe bond formation. The total energy barrier for vacancy-assisted dissociation is 0.63 eV with respect to the minimum-energy adsorption state, and is less than that in a clean surface (0.78 eV) and will certainly facilitate dissociation of CO. However, though this reduction in energy barrier is not large, Figure 5 reveals a number of reasons for dissociation of CO being more efficient in the vicinity of a vacancy defect. First, the vacancy allows the C atom to penetrate to subsurface and therefore, if a comparison with clean surface without vacancy is to be made,

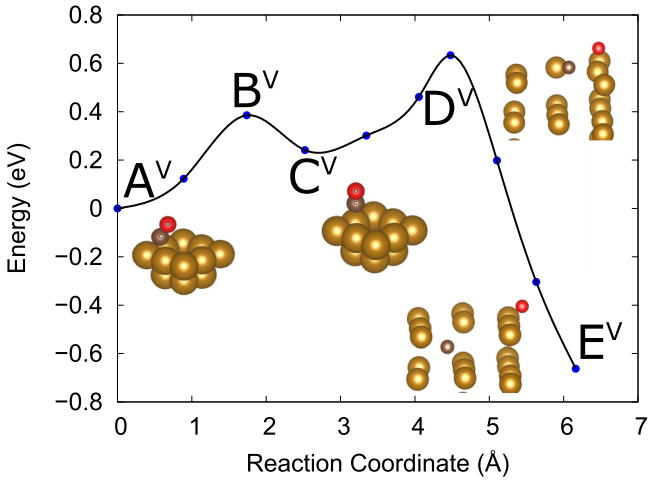


FIG. 5. Minimum energy path for CO dissociation in the presence of a vacancy defect on the surface. Starting from the quasi-threefold site-adsorbed configuration, the first barrier with saddle point $B^V$ appears from migration of the CO molecule to the less stable vacancy-nearest neighbour on-top site $C^V$. From this configuration the C and O atoms are decomposed via a transition state $D^V$ to the final configuration $E^V$ where the C atom is 0.6 Å deep in the vacancy and the O atom is adsorbed on the surface away from the vacancy.

surface-to-subsurface diffusion on clean surface must also be taken into account as a process of immediate succession. Second, the actual dissociation process starts from the nearest neighbour on-top site, with respect to which the barrier is only 0.39 eV; the first part A → C in the energy path (Figure 5) corresponds to molecular migration of CO. Third, the reverse barrier to the more stable quasi-threefold site is 0.14 eV. Therefore, a higher CO-coverage increases the probability that the on-top nearest neighbour site is occupied and will dissociate to a state 0.9 eV lower with respect to it. Finally, the reverse barrier for dissociation is a large 1.4 eV, which makes it difficult for the C atom to react with C atom to go back to a CO-molecular state. The reverse barriers for CO dissociation in H, O, and OH pre-covered surfaces calculated by Liu *et al.*[15] are often larger than 1.5 eV. The effect of vacancies on these adsorbates is unknown but given the large reverse barrier on clean surface, it is unlikely that the reaction between these adsorbates (H, O, or OH) with C atom trapped in a surface vacancy will be favourable either.

### Surface to subsurface diffusion of C

Carbon surface to subsurface diffusion is an integral part of the carburisation process. Unlike a surface vacancy, that naturally allows the C atom to penetrate to the subsurface, the dynamics of the C atom moving towards the subsurface from a clean surface is complicated and involves indirect pathways. The C atom must diffuse to a subsurface octahedral interstitial site to achieve an energetically stable state. Figure 6 shows the diffusion path for surface to subsurface diffusion of C with (top panel) or without O atoms (bottom panel) as surface adatoms. In earlier studies the surface to subsurface diffusion of C was calculated as a standalone event[16] with a single C atom. We recalculated this diffusion barrier using a

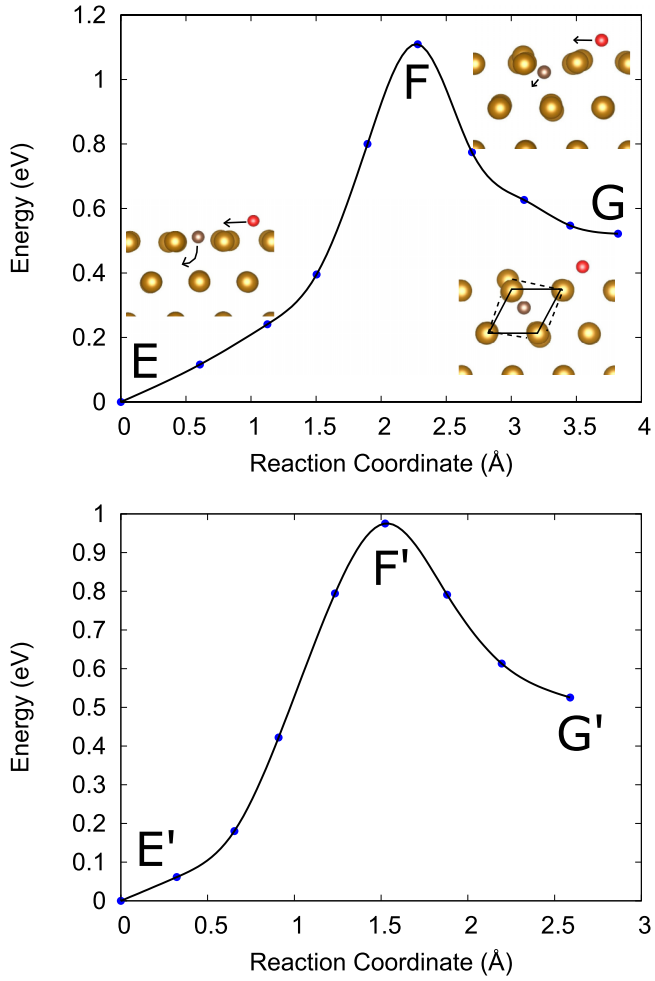


FIG. 6. Minimum energy paths for surface to subsurface diffusion of C on clean 110 surface. Top: Diffusion in the presence of O atom on the surface. The initial minimum E is identical to the final minima of Figure 4. The arrow marks the creep path of the O atom. Bottom: Diffusion without the presence of O atom. Note that the barrier at F′ is 0.97 eV lower than that with an O adatom (1.16 eV) even though the energy difference between the initial and the final configuration is almost same (~0.5 eV). Note that similar works with surface to subsurface diffusion without O, shown in the bottom panel, have been previously published.[16] It has been recalculated here with a more dilute coverage to estimate the effect of the O adatom (top panel).

larger supercell with a lower coverage of 0.0625 ML, which yielded a slightly lower barrier of 0.97 eV, in comparison to the 1.18 eV computed by Jiang *et al.*[16] with a 0.111 ML coverage. This is coherent with our earlier observation of the reduction of dissociation barrier of CO as the coverage is decreased.[28] However, in practice, the surface to subsurface diffusion of C is most likely to be a follow up process of the dissociation of a hydrocarbon, which, in this case is CO, the O atom will remain on the surface as a byproduct unless it desorbs by reacting with another CO molecule to form $CO_2$ or with an external reactant such as H or S. Figure 6 shows that the presence of an O atom on the surface has a large impact on the energy barrier of the diffusion of C. It is not difficult to explain the role of oxygen in raising the energy barrier and is attributed to the high electron affinity of the O atom. In a similar manner discussed in dissociation, the presence of the O in the vicinity reduces the electronic overlap of the Fe–C covalent bonds, therefore

restricting the dynamics of the C atom. Furthermore, it is shown by the arrows in Figure 6 that the O atom does not remain in a stable adatom site for the duration of the diffusion of C but moves slightly towards the C atom as if following the C atom. This creep of the O atom on the surface is the result of electron sharing between C and O atom in the electron-deficit vacancy environment even after the C–O bond is severed. The transition state for the diffusion is therefore strongly influenced by the O atom, increasing the diffusion barrier. With the O surface adatom present, the diffusion barrier is estimated to be 1.16 eV but is only 0.97 eV when the O adatom is discarded. This energy difference, i.e., 0.2 eV is small, but can still make a significant difference in terms of the qualitative preference of C diffusion with or without the presence of O adatoms, when there is no other activator present except thermal excitation. The magnitude of the zero-point energy correction for these systems is typically 0.02-0.03 eV[43] and should not affect these results. Since both calculations, with and without O adatom are calculated using the exact same base system with identical DFT parameters, a qualitative claim can be made that the C diffusion is advantageous without the O adatom. The practical implication of this observation is that the removal of the O atom after CO-dissociation by reaction with another reactant such as H or S is beneficial for a higher yield of the carburisation process.

## DISCUSSION

In the sections titled "Adsorption" and "Dissociation," we have observed that in the presence of a vacancy defect on the surface, there are two competing interactions that affect the consecutive processes of carburisation, i.e., adsorption and dissociation of CO, followed by surface-to-subsurface diffusion of C. These interactions are (1) the attractive interaction between a vacancy defect and a C atom that enhances the C–Fe bond within the vacancy, and (2) the large electron-affinity of O that weakens the C–Fe bond in the vicinity of a vacancy. The first phenomenon increases adsorption energies, reduces dissociation and diffusion barriers, while the second one reduces the adsorption energies and increases energy barriers for dissociation and diffusion in the vicinity of a vacancy. Therefore in order to understand the role of vacancy defects in carburisation, we must understand the nature of these two competing interactions. We know from previous works that the vacancy in bulk Fe acts as a C-trap with a binding energy close to 0.64 eV.[5,29] The binding energy represents the energy cost to displace the C atom away from the vacancy to a bulk octahedral interstitial site, which is the most stable site for a C interstitial.[5] We calculate the binding energy of a lone C atom with a surface vacancy with respect to a C adatom on the clean surface. This can be estimated by Eq. (2),

$$\Delta E^V(C) = [E^V(C) - E^{cln}(C)] - [E^V - E^{cln}], \qquad (2)$$

where $E^{cln}$ is the total energy of a clean Fe surface, $E^{cln}$ (C) is the total energy of clean Fe surface with C adatom at hollow site as the most stable adatom site for C, $E^V$ is the total energy of a surface with vacancy and $E^V$ (C) is the total energy of a surface with vacancy, and a C atom in the vacancy. The magnitude of $\Delta E^V(C)$ is estimated to be 1.71 eV in our calculation, suggesting a strong binding between C and a surface vacancy with respect to C as a surface adatom at the on-top site. In practice, however, the C adatom is the product of a metal-hydrocarbon reaction and, in this particular instance, CO, and does not get adsorbed on the surface on its own. A lone C adatom at the on-top site is assumed here as a reference point in the vicinity of the defect in order to estimate the extent of the C-vacancy binding in the absence of an oxygen atom and thus gain an insight into the role of O and C atoms separately. This helps us understand the transition state for CO-dissociation where the two atoms get separated. The large C-vacancy binding energy lowers the dissociation barrier and competes with the energy hike due to uncompensated electron affinity of O in the electron-deficit vicinity of the vacancy defect.

Table II shows the individual adsorption energies for the C and O atoms at different adsorption sites. The adsorption energies are calculated relative to the minimum energy site to avoid numerical errors. Note that the energy of the C atom adsorbed on the on top site in the presence of vacancy is +0.84 eV relative to the minimum-energy adsorption configuration, i.e., the vacancy site itself, while in an on-top site far away from the vacancy, it is calculated as +1.71 eV, using Eq. (2). This suggests that it is energetically more favourable for the C atom to move closer to the vacancy. Also the adsorption of the O atom near a vacancy defect is energetically unfavourable due to the electron deficit atmosphere in the vicinity of the vacancy.

The electronic localization function is plotted using the VNL visualisation package[50] on the XY planes parallel to the surface at different planes to highlight the electron distribution and covalent bonds with the O and C atoms dissociated on the surface. In Figure 7, Panel 1 shows a large localization of an electron at the O atom next to the electron deficit vacancy cavity. Panel 2 shows the same system but is plotted at the plane with the C atom. Note that the C atom is 0.6 Å deep

TABLE II. Adsorption energies relative to the respective minimum-energy adsorption site for individual C and O atoms at different surface adsorption sites. All energies are given in eV.

| | Clean surface | | | | | |
|---|---|---|---|---|---|---|
| | On-top | Hollow | Bridge | QTF[a] | | |
| C | 1.54 | 0 | 1.08 | 0.03 | | |
| O | 0.87 | 0 | 0.54 | 0.02 | | |
| | Surface with vacancy defect | | | | | |
| | On-top′[b] | Hollow | Bridge | QTF | On-top″[c] | Vacancy |
| C | 0.84 | 0[d] | 0.69 | 0[d] | 1.14 | 0 |
| O | 0 | 1.21 | 0.66 | 1.15 | 0.47 | 1.41 |

[a]Quasi-threefold.
[b]On-top, nearest neighbour to the vacancy.
[c]On-top, 2nd nearest neighbour to the vacancy.
[d]Relaxed to vacancy.

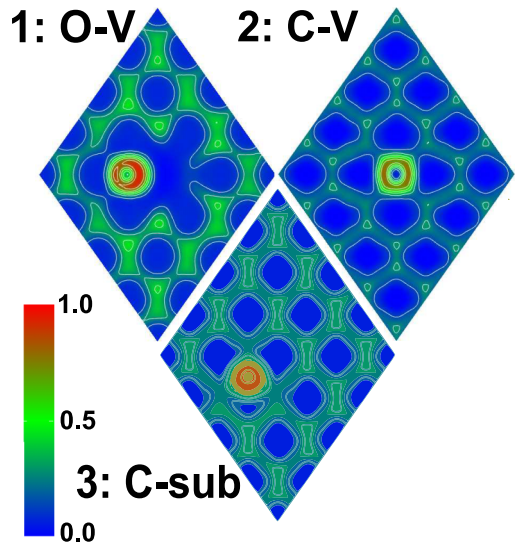


FIG. 7. Visualization of the electronic localization function at different layers for the dissociated state. Panel 1: At the O atom with C dissociated and adsorbed in the vacancy. Panel 2: At the C atom at the vacancy for the same system. Panel 3: For a single C atom in the subsurface interstitial site. Note that the electron localization at the O atom is much higher and that at the C atom is well spread. The bond is very different from that for the C atom at a subsurface interstitial site, for which, the excess electron is more localized.

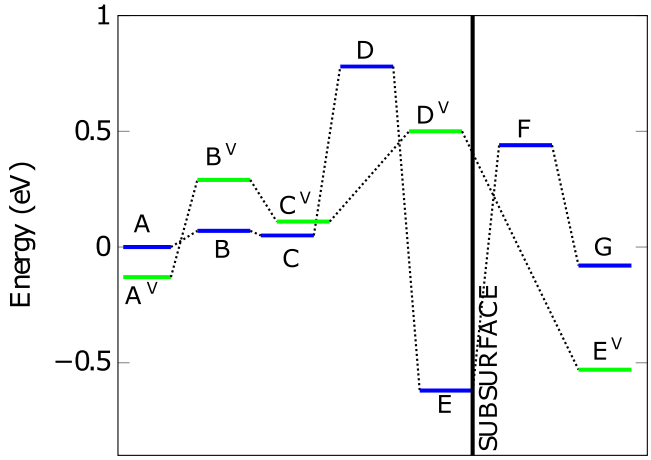


FIG. 8. Comparison of the minimum energy paths for CO dissociation in the presence of a vacancy (green) with the combined energy paths of dissociation, followed by surface to subsurface C-diffusion on clean surface (blue). The different states are labeled in coherence with actual reaction paths in Figures 4, 6, and 5. The energy states in the presence of a vacancy are differentiated with superscript $V$. The energy A of the initial configuration in Figure 4, i.e., a CO molecule adsorbed on the clean surface, is set as the reference level. Note that the combined clean surface reaction path is associated with a much larger, 11 Å reaction displacement, in comparison to that of the vacancy-dissociation path, 6.2 Å.

in the surface and forms symmetric covalent bonds with four Fe atoms in the same layer. The bond with a 5th Fe atom at the 2nd layer is weak. However, for a lone C atom in a subsurface octahedral interstitial with a structure shown as the final configuration in Figure 6, the C atom forms covalent bonds with 6 Fe atoms. Finally, Panel 3 shows three of the 6 Fe atoms that built the octahedral cage, the other three Fe atoms are in the 2nd layer. The amplitude of electron localization is much higher without the presence of O atom as the excess electrons are localized in the C atom only.

A side-by-side comparison between the energy paths of the vacancy-assisted dissociation and combined dissociation and surface-to-subsurface diffusion is made in Figure 8. Although the two reaction paths appear similar at first glance in terms of positioning of the minor and major energy barriers separated by intermediate minima, the corresponding mechanisms are entirely different. The initial state for the clean surface A represents a configuration where the CO molecule is adsorbed on the surface. This state is chosen as the reference system for Figure 8 and all energies in that figure are measured with respect to it. The initial state for the surface with a vacancy defect, $A^V$, is the minimum energy adsorption configuration in the presence of a vacancy. In this configuration, the adsorption energy of CO next to a vacancy is favourable by an energy of 0.13 eV than the most favourable adsorption configuration for clean surface (see Table I). Therefore $A^V$ is 0.13 eV lower than the reference system A. The reaction path associated to the dissociation of CO, followed by surface-to-subsurface diffusion of carbon on clean surface (blue lines in Figure 8), reaches a low energy dissociated state E by crossing a primary barrier of 0.78 eV at the transition state D. The reaction coordinate, which represents the summed displacement of all atoms during the reaction process, is 7.2 Å for the CO dissociation only. A significant part of this displacement comes from the migration of a molecular CO from the most favourable adsorption site to another metastable site to initiate dissociation. Relaxation of the neighbouring Fe lattice also contributes to the large displacement as defined by the reaction coordinate. A further 3.8 Å is required for the carbon atom to reach the subsurface, which is achieved by crossing another barrier ($F$) of 1.16 eV with respect to the dissociated state. It is highly likely that once the system falls into the deep dissociated state $E$, it will be stabilised there, unable to overcome the barriers on both sides, 1.5 eV and 1.16 eV, respectively. On the other hand, in the presence of vacancy, both of the subsequent processes, i.e., dissociation, followed by subsurface diffusion, are complete within the pathway $C^V \rightarrow D^V \rightarrow E^V$. The total atomic displacement is only 6.2 Å in the presence of the vacancy and is much smaller than that of the combined dissociation and subsurface diffusion on clean surface, 11 Å. A large relaxation of neighbouring Fe atoms causes the dissociation barrier to rise in higher coverages.[28] In an earlier work, we have shown that the larger the relaxation in the Fe atoms, the further the elastic deformation propagates and for higher coverages, this elastic deformation influences the C-adsorption in neighbouring sites raising the effective dissociation barrier.[28] Note that the reverse barrier $E^V \rightarrow D^V$ for vacancy-assisted dissociation is also as high as 1.3 eV. Therefore, in either case, once the CO molecule is dissociated, it faces a large activation barrier to go back to its gaseous state. The highest transition state represents the dissociation barrier and is lower for the vacancy-surface by ~0.3 eV. We see that, despite a large C-vacancy binding energy of 1.7 eV, due to the counter-interaction by the O atom, the energetic advantage of vacancy-assisted dissociation is not large. However, as we have pointed out earlier, there are certain reasons for sustained carburisation to more likely occur on defected surface and are listed here. First, the adsorption energy is higher at the edge

of the vacancy, therefore the probability is higher than the CO molecule gets adsorbed in those sites, than on a clean surface site. On a surface exposed to the reacting gasses, it is expected that defects are present randomly. Therefore from an atomistic perspective, the adsorbate gas molecules react with both a clean and vacancy-defected surface. The negative initial energy for the defect system indicates a lower adsorption energy which will draw the adsorbate to be adsorbed next to a vacancy defect. Second, the molecular migration path is smaller and the relaxation of Fe atoms is much less for the vacancy-assisted dissociation. This will reduce the time consumed for the dissociation/diffusion process to complete. Third, most importantly, the vacancy allows the C atom to diffuse into the subsurface layer without a secondary diffusion barrier. On the other hand, for clean surfaces, when the CO molecule is dissociated, the system retains a deep energy state and the C atom has to cross another 1.16 eV barrier to diffuse to the subsurface layer.

## CONCLUSIONS

First-principles DFT calculations were conducted to investigate carburisation of steel with CO through the characterisation of CO adsorption and dissociation, followed by surface to subsurface diffusion of C on Fe-110 surface. The role of a single vacancy defect on these processes is studied with energetics calculations and electronic structure analysis. The creation of a single vacancy on the Fe-110 surface is found to be energetically inexpensive with a low formation energy and therefore is likely to be abundant. Adsorption of CO is estimated to be slightly favourable on sites at the edge of the vacancy but highly unstable at the vacancy site itself. CO-dissociation paths and C-diffusion paths are calculated using climbing-image nudged elastic band method. A lower dissociation barrier appears when a vacancy is present. Computation on the energetics and charge density analysis shows that there are two competing factors acting on the dissociation process in the presence of the vacancy: (1) the strong C-vacancy attractive interaction that helps lowering the CO dissociation barrier and (2) the high electron affinity of the O atom renders the O-adatom site unstable in the electron-deficit vicinity of the vacancy defect, increasing the transition state energy. However, the effective dissociation barrier is low provided that the O atom moves away from the vacancy, while the C atom gets adsorbed in the vacancy cavity. Furthermore, unlike the clean surface the vacancy defect also allows the dissociated C atom to penetrate to the subsurface layer without crossing another energy barrier. Considering the overall process of carburisation consists of consecutive processes, i.e., adsorption, dissociation, and surface-to subsurface diffusion of C, we show that in the presence of a vacancy defect on the surface, carburisation is energetically more favourable than on a clean surface. With these results in hand, it is now possible to consider C diffusion and segregation in the subsurface and in the presence of other extended defects such as grain boundary, a project that is currently underway.

## ACKNOWLEDGMENTS

This work is supported by the Qatar National Research Fund (QNRF) through the National Priorities Research Program (Grant No. NPRP 6-863-2-355). The advanced computing facility of Texas A&M University at Qatar is used for all calculations.

## APPENDIX A: CHOICE OF SURFACE SUPERCELL WITH A VACANCY DEFECT

In order to compute a precise value of the defect formation energy, the unwanted energy contribution from the periodic boundary condition must be eliminated. This problem is usually tackled by using correction schemes[51,52] but for the present case of a surface where adsorbate atoms are present, the correction becomes complicated and a standardized scheme is still missing. Therefore we chose the simpler approach of choosing the smallest supercell large enough to minimize computer time while ensuring that the interaction between the defect periodic images is negligibly weak. To do this, we calculated the formation energy of a single Fe vacancy on the surface using a number of different supercells. Figure 9 shows the formation energy as a function of the surface area. The thickness of the slab is fixed. The total computational cost in CPU-seconds is shown for each supercell. It is clear that for surfaces larger than $4 \times 4$, the change in the formation energy becomes negligible while the computational cost increases dramatically.

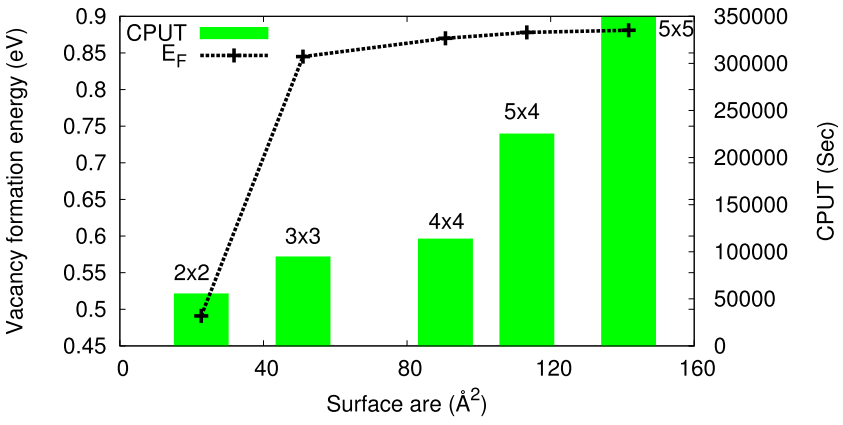


FIG. 9. Formation energy of a surface vacancy as a function of surface area limited by the periodic boundary condition of the DFT calculation. Columns show total computer-time to calculate the formation energy.

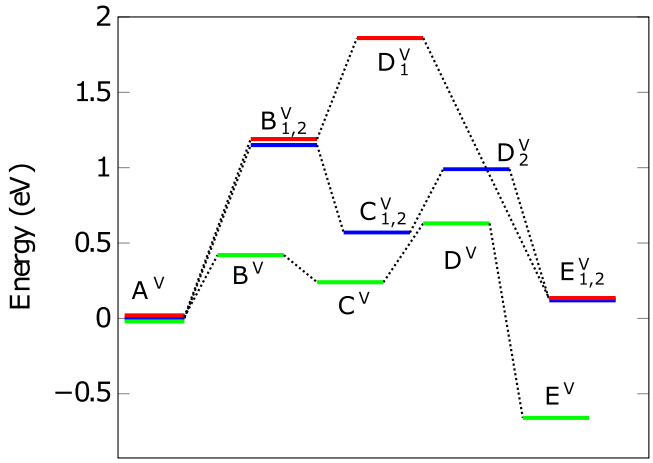


FIG. 10. Energy paths for CO dissociation in the presence of a vacancy. Energy states are shown for the three different dissociation paths observed in this work. The green line depicts the minimum energy path and corresponds to Figure 5. The energy states associated with the other two paths are denoted with indices 1 and 2. $A^V$ is the initial minimum—the quasi-threefold adsorption configuration and is universal for all energy paths. $E^V$ and $E^V_{1,2}$ are the two final minima. Intermediate minima and transition states are marked with C and D, respectively.

## APPENDIX B: DIFFERENT ENERGY PATHS FOR CO DISSOCIATION

Figure 10 depicts three possible energy paths for dissociation in the presence of a surface vacancy, including the minimum-energy path (green) corresponding to Figure 5. The minimum energy path appears only when the O atom dissociates to a neighbouring quasi-threefold adatom site further away from the vacancy.

[1]A. Vehanen, P. Hautojärvi, J. Johansson, J. Yli-Kauppila, and P. Moser, Phys. Rev. B **25**, 762 (1982).
[2]D. Johnson and E. Carter, J. Phys. Chem. **114**, 4436 (2010).
[3]K. Sato, Q. Xu, D. Hamaguchi, S. Huang, and T. Yoshiie, J. Phys.: Conf. Ser. **443**, 012031 (2013).
[4]T. Iwai, Y. Ito, and M. Koshimizu, J. Nucl. Mater. **329**, 963 (2004).
[5]C. Domain, C. S. Becquart, and J. Foct, Phys. Rev. B **69**, 144112 (2004).
[6]Y. Fukai, K. Mori, and H. Shinomiya, J. Alloys Compd. **348**, 105 (2003).
[7]C.-C. Fu, J. Torre, F. Williame, J.-L. Boucquet, and A. Barbu, Nat. Mater. **4**, 68 (2005).
[8]M. Kabir, T. Lau, D. Rodney, S. Yip, and K. van Vilet, Phys. Rev. Lett. **105**, 095501 (2010).
[9]D. Tanguy and M. Mareschal, Phys. Rev. B **72**, 174116 (2005).
[10]Q. Zhang, B. Han, K. Heier, J. Li, J. Hoffman, M. Lin, A. Derecskei-Kovacs, and H. Cheng, J. Phys. Chem. C **115**, 12068 (2011).
[11]E. Pippel, J. Woltersdorf, and R. Schneider, Mater. Corros. **49**, 309 (1998).
[12]D. Young, J. Zhang, C. Geers, and M. Schütze, Mater. Corros. **62**, 7 (2011).
[13]Q. Zhang, B. Han, X. Tang, K. Heier, J. Li, J. Hoffman, M. Lin, S. Britton, A. Derecskei-Kovacs, and H. Cheng, J. Phys. Chem. C **116**, 16522 (2012).
[14]D. Jiang and E. A. Carter, Surf. Sci. **570**, 167 (2004).
[15]S. Liu, Y.-W. Li, J. Wang, and H. Jiao, J. Phys. Chem. C **119**, 28377 (2015).
[16]D. Jiang and E. A. Carter, Phys. Rev. B **71**, 045402 (2005).
[17]A. Stibor, G. Kresse, A. Eichler, and J. Hafner, Surf. Sci. **507–510**, 99 (2002).
[18]R. Sanderson, *Polar Covalence* (Academic Press, Inc., 1983).
[19]L. Gonzalez, R. Miranda, and S. Ferrer, Surf. Sci. **119**, 61 (1982).
[20]G. Wedler and H. Ruhmann, Surf. Sci. **121**, 464 (1982).
[21]G. Wedler and H. Ruhmann, Appl. Surf. Sci. **14**, 137 (1983).
[22]M. Elahifard, M. Jigato, and J. Niemantsverdriet, Chem. Phys. Chem. **13**, 89 (2012).
[23]S. Booyens, M. Bowker, and D. J. Willock, Surf. Sci. **625**, 69 (2014).
[24]T. Wang, X. Tian, Y.-W. Li, J. Wang, M. Beller, and H. Jiao, J. Phys. Chem. C **118**(2), 1095 (2014).
[25]X. Tian, T. Wang, Y. Yang, Y.-W. Li, J. Wang, and H. Jiao, J. Phys. Chem. C **118**(35), 20472 (2014).
[26]S. A. Roncancio, D. H. Linares, H. A. Duarte, G. Lener, and K. Sapag, Am. J. Anal. Chem. **6**, 38 (2015).
[27]T. Wang, X. Tian, Y.-W. Li, J. Wang, M. Beller, and H. Jiao, ACS Catal. **4**(6), 1991 (2014).
[28]A. Chakrabarty, O. Bouhali, N. Mousseau, C. S. Becquart, and F. El-Mellouhi, "Insights on finite size effects in Ab-initio study of CO adsorption and dissociation on Fe 110 surface," J. Appl. Phys. (to be published); preprint arXiv:1603.04662 [physics.comp-ph].
[29]O. Restrepo, N. Mousseau, F. El-Mellouhi, O. Bouhali, M. Trochet, and C. S. Becquart, Comput. Mater. Sci. **112**, 96 (2016).
[30]J. Perdew, J. Chevary, S. Vosko, K. Jackson, M. Pederson, D. Singh, and C. Fiolhais, Phys. Rev. B **46**, 6671 (1992).
[31]J. Perdew, K. Burke, and M. Ernzerhof, Phys. Rev. Lett. **77**, 3865 (1996).
[32]J. Perdew, S. Kurth, A. Zupan, and P. Blaha, Phys. Rev. Lett. **82**, 2544 (1999).
[33]B. Hammer, L. Hansen, and J. K. Norskov, Phys. Rev. B **59**, 7413 (1999).
[34]B. G. Janesko, Top. Curr. Chem. **365**, 25 (2015).
[35]S. Kurth, J. Perdew, and P. Blaha, Int. J. Quantum Chem. **75**, 889 (1999).
[36]G. Henkelman and H. Jónsson, J. Chem. Phys. **113**, 9901 (2000).
[37]G. Ackland, D. Bacon, A. Calder, and T. Harry, Philos. Mag. A **75**, 713 (1997).
[38]C. Domain and C. S. Becquart, Phys. Rev. B **65**, 024103 (2001).
[39]P. Korzhavyi, I. Abrikosov, and B. Johansson, Phys. Rev. B **59**, 011693 (1999).
[40]H. Sugimoto and Y. Fukai, Acta Mater. **67**, 418 (2014).
[41]G. Kresse and J. Hafner, Phys. Rev. B **47**, 558 (1993).
[42]S. Grimme, J. Comput. Chem. **27**, 1787 (2006).
[43]D. Jiang and E. A. Carter, Phys. Rev. B **67**, 214103 (2003).
[44]M. Acet, H. Zähres, E. F. Wassermann, and W. Pepperhoff, Phys. Rev. B **49**, 6012 (1994).
[45]P. Bloński and A. Kiejna, Surf. Sci. **601**, 123 (2007).
[46]M. Spencer, A. Hung, I. K. Snook, and I. Yarovsky, Surf. Sci. **513**, 389 (2002).
[47]H. Schaefer, K. Maier, M. Weller, D. Herlach, A. Seeger, and J. Diehl, Scr. Metall. **11**, 803 (1977).
[48]L. DeSchepper, D. Segers, L. Dorikens-Vanpraet, M. Dorikens, G. Knuyt, L. Stals, and P. Moser, Phys. Rev. B **27**, 5257 (1983).
[49]W. Erley, J. Vac. Sci. Technol. **18**, 472 (1981).
[50]See www.quantumwise.com for Virtual NanoLab version 2015.1, QuantumWise A/S.
[51]G. Makov and M. Payne, Phys. Rev. B **51**, 4014 (1995).
[52]C. Freysoldt, J. Neugebauer, and C. van de Walle, Phys. Rev. Lett. **102**, 016402 (2009).